Recent progress of diamond device toward power application

Julien Pernot, Gauthier Chicot, Alexandre Fiori, Aboulaye Traoré, Thu Nhi Tran Thi, Pierre-Nicolas Volpe, David Eon, Franck Omnès, Etienne Bustarret, Etienne Gheeraert, et al.

RECENT PROGRESS OF DIAMOND DEVICE TOWARD POWER APPLICATION

J. Pernot*, G. Chicot, A. Fiori, A. Traoré, T.N. Tran Thi, P.N. Volpe, D. Eon,
F. Omnès, E. Bustrarret, E. Gheeraert and P. Muret

Institut Néel, CNRS and Université Joseph Fourier, BP166, 38042 Grenoble Cedex 9, France
* E-mail: julien.pernot@grenoble.cnrs.fr

ABSTRACT

The state of the art of the Institut Néel research activity in the field of diamond power devices will be described and discussed. The active layers of the device are based on boron-doped monocristalline (100) diamond (with doping level varying between 10^{14} to 10^{21} cm^{-3}) grown on Ib high temperature high pressure (HPHT) diamond substrate. The progresses done on diamond/metal interface, diamond/dielectric interface, or sharp gradient doping, permit recently the fabrication of original structures and devices, which will be detailed here (Schottky diode, boron doped δ-FET and MOS capacitance).

1. INTRODUCTION

The high breakdown electric field, the elevated mobility and the outstanding thermal conductivity make diamond the ultimate semiconductor for high power and high frequency applications (see Table 1). In low-doped diamond, the acceptor (i.e. Boron) and donor (i.e. phosphorus) dopant atoms have a low ionization rate, due to high ionization energy (0.38 eV and 0.57 eV respectively), resulting in resistive material and consequently high serial resistance for devices. In order to get around this problem, news devices concept must be proposed for the fabrication of high power electronic switches (i.e. transistor or diode) based on diamond materials.

Field Effect Transistor (FET) solutions based on 2D hole gas are now under investigation: i) FET based on hydrogen terminated diamond surface [1-3], ii) FET based on AlN/diamond hetero-structure [4], iii) FET based on boron δ-doping concept (δ-FET) [5-7]. For the Si technology, the classical way to perform such 2D gas is the use of a MOS capacitance. Diamond Schottky or *pn* junction diodes are also investigated by several groups for high power applications [8-12]. The unipolar or bipolar devices generally include a highly boron doped diamond layer in the stacked structure (metallic B-doped epilayer or substrate below the low B-doped layer in the case of Schottky diode). The main problem of such stacked structure is to combine a high breakdown voltage in the reverse regime (due to the highly doped layer) with a high current density in the forward regime (due to the low doped layer). Based on the control of the low B-doping level (10^{15}-10^{16} cm^{-3}) [1] as well as the highly B-doping of diamond (more than 5×10^{20} cm-3), and also on recent progresses done in the diamond interfaces (metal, dielectric, or sharp gradient doping), original structures and devices have been recently performed and characterized at the Institut Néel (like Schottky diode, boron doped δ-FET and MOS capacitance) [5,6,11-14].

In this work, the state of the art of the Institut Néel

Property	Symbol [unit]	Si	GaAs	4H-SiC	GaN	Diamond
Bandgap	E_G $[eV]$	1.1	1.43	3.23	3.45	5.45
Saturated drift velocity	v_S $[10^7\ cm/s]$	1.0	1.0	2.0	2.2	1.1
Electron mobility	μ_n $[cm^2/V.s]$	1500	8500	1000	1250	1000
Hole mobility	μ_p $[cm^2/V.s]$	480	400	100	200	2000
Breakdown field	E_B $[MV/cm]$	0.3	0.4	3	2	10
Relative dielectric constant	ϵ_r	11.8	12.5	9.8	9	5.5
Thermal conductivity	λ $[W/cm.K]$	1.5	0.5	5	1.5	22
Johnsons figure of merit	JFM $[10^{23}\ \Omega.W/s^2]$	2.3	4	900	490	2530
Keyes figure of merit	KFM $[10^7\ W/Ks]$	10	3.3	53	17	218
Baligas figure of merit	BFM [Si=1]	1	14	554	188	23068

TABLE I. Basic physical properties of wide band gap semiconductors and related figures of merit[1] (Johnson, Keyes and Baliga) (see footnote for definitions).

[1] Johnson's figure of merit: $JFM = (\frac{E_B v_S}{2\pi})^2$ - Frequency and power products of transistor.
Keyes' figure of merit: $KFM = \lambda(\frac{c v_S}{2\pi\epsilon_r})^{\frac{1}{2}}$ - Thermal limitation on high-frequency performance.
Baliga's figure of merit $BFM = \epsilon_r \mu E_B^3$ - Loss in high power and high-frequency operation.

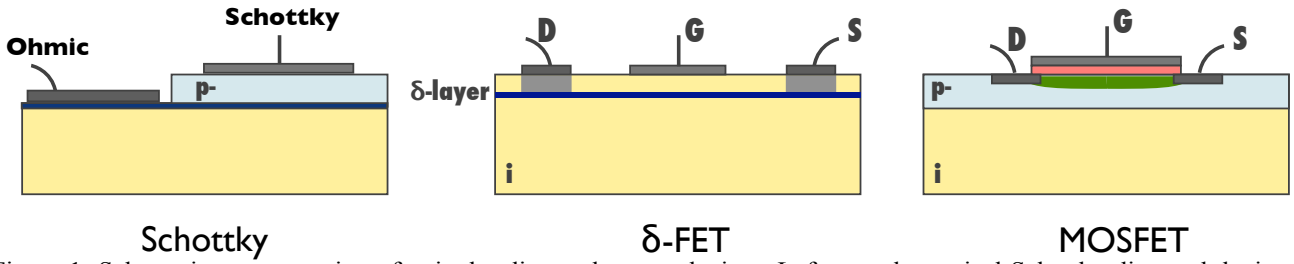

Figure 1: Schematic representation of unipolar diamond power devices. Left: pseudo-vertical Schottky diamond device, the ohmic contact is deposited on a highly doped *p*-type layer after etching. The Schottky metal is deposited on an oxidized diamond surface. Middle: Boron δ-doped FET: a highly doped layer (metallic [B]>5×10^{20} cm^{-3}) between two intrinsic layers, the source (S) and drain (D) are ohmic contacts allowing access to the degenerated channel. Right: MOSFET structure: Al/Al_2O_3/*p*-type diamond as the gate (G) of the MOS capacitance.

research activities in this field is reported. The first part of the work will be dedicated to the Schottky diode, the second to the δ-FET, the third to the MOS capacitance (see Fig. 1), and, finally the last to a summary.

2. DIAMOND SCHOTTKY DIODE

Homoepitaxial diamond has been recognized by Landstrass et al.[15] as the semiconductor having the highest breakdown electric field of at least 20 MV/cm, much larger than in other wide band gap semiconductors. This property, associated to its high thermal conductivity and high carrier mobility, makes diamond the ultimate semiconductor for high power and high voltage rectifiers (like Schottky diode).

In this work, homoepitaxial diamond layers have been prepared on 3×3 mm^2, (100) oriented Ib substrate, by microwave plasma enhanced chemical vapor deposition in a silica reactor with 4% of CH_4 in hydrogen under a pressure of 30 torr and a temperature of 830 °C, without intentional introduction of boron. The roughness of the substrate was measured by atomic force microscopy to be 2–5 nm rms. Schottky contacts with a diameter of 150 μm have been achieved by gold deposition through holes in a metallic mask on the epilayer surface treated by ozone produced by VUV light as described in Ref. 16. Four Ti/Au Ohmic contacts were deposited and annealed 1 h at 750 °C in the corners of the sample after an acid cleaning of the surface, before VUV ozone treatment and Schottky metallization. I-V characteristics of the Schottky diodes have been studied on the one hand at low voltages in the as-grown epilayer, after a first anneal at 750 °C 10 min. and a second anneal at 825 °C 1 h, both under vacuum, and on the other hand under several kilovolt reverse voltages, without reaching avalanche breakdown [13]. In between each annealing process, Schottky metal deposits are removed by chemical treatment, and then deposited again after a new VUV ozone treatment. After each anneal, the current level increases in the whole voltage range, both in forward and reverse bias. As the hydrogen concentration in the as-grown epilayer initially amounted up to 8×10^{19} cm^{-3}, above the SIMS detection limit of 10^{19} cm^{-3}, the subsequent anneals have depassivated the boron acceptors which were previously passivated by hydrogen, like found in Ref. 17. It is statistically probable that BH complexes leading to deep levels [18] can form readily when the concentration of hydrogen is more than three orders of magnitude larger than that of boron, even if the growth temperature is above that known for BH pairs dissociation when the concentration of the two species are of same magnitude. The net ionized acceptor concentration increased as well as the electric field in the space charge zone, inducing an increase of the current levels. Moreover, the potential barrier height grew by about 1V after the second anneal. This fact was not expected if the Fermi level position would have stayed the same because of an unchanged metal-diamond interface. But it is known that hydrogen trapped into the subsurface atomic layers of diamond induces an electrical dipole which decreases the effective barrier height by about 1V [19], as found experimentally here again. Consequently, one must conclude that the second anneal has decreased the sub-surface hydrogen concentration.

Only after the second anneal, it became possible to probe the depletion zone thickness and net ionized acceptor charge by C-V measurements. They were performed with an Agilent E4980A bridge at a frequency of 1.2 kHz and a temperature of 400 K, well below the cut-off frequency of the diode, with the help of a special circuit and external source allowing dc biasing up to 800 V. The width *w* of the space charge zone and therefore the probed depth was deduced. The net acceptor concentration N_A-N_D was then calculated. The net acceptor concentration appears as not constant, fluctuating between 2.5×10^{14} and 4×10^{15} cm^{-3}, because of a residual passivation of boron by hydrogen in the first 6 μm of the epilayer [12]. Then, it reaches 3×10^{16} cm^{-3} between depths of 6.7 and 7.7 μm.

The current-voltage characteristics of several diodes were investigated with the help of four different experimental setups, which provided increasing maximum voltages along five runs, which took place in a period of 15 months after the last sample processing. The I(V) characteristics are summarized in Fig. 2 and detailed in Ref [12]. The measurement of Fig. 2a) was performed in vacuum, ten months after fabrication, and displayed an avalanche breakdown at 7.5 kV with current densities comparable to that given in Ref. 17. A new measurement run was performed in the same setup, 13 months after

fabrication, on another diode, which withdrew almost 10 kV before avalanche breakdown Figs. 2b) and 2c).

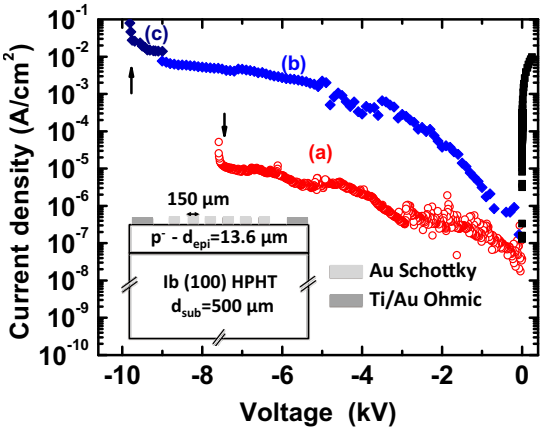

Figure 2: Current density as a function of voltage under vacuum in two Schottky diodes (a–c). (a) and (b) characteristics have been recorded with a ramp voltage of 5 V/s while (c) has been recorded manually. Arrows delineate avalanche breakdown voltages. A schematic cross section of the structure of the sample is drawn.

Using two-dimensional simulations, achieved with the software « SENTAURUSTCAD » and the parameters deduced from the diode geometry and doping profile, the electric field is evaluated to be 7.5 MV/cm at the center of the diode [12].

According to the results and analysis presented in this study, it can be concluded that diamond homoepitaxial layers are able to withstand electric fields in the range predicted in Ref. 15 before avalanche breakdown, far higher than those known in all other semiconductors, provided an oxidation process of the surface resulting in superior electrical and chemical passivations efficiencies has been applied. These findings open the route for implementing high voltage diodes and other unipolar electronic devices. The next investigations will be focused on the optimization of the structure in order to achieve Schottky diodes, which are able to maintain more than few kV in reverse regime and with a forward current density larger than 100 A/cm^2. To perform such structure, highly B-doped diamond must be stacked below the low doped layer (as shown on Fig 1(a) - this is not the case of the sample analysed in this work) or directly grown on a highly B-doped substrate.

3. DIAMOND FIELD EFFECT TRANSISTOR

Due to outstanding physical properties (large carrier mobility, high breakdown voltage, exceptional thermal conductivity), diamond is the ultimate semiconductor for high power and high frequency FET. These features should in principle allow developing new electric switches with low loss. One difficulty is that because of the high ionization energy of the boron *p*−type dopant, the equilibrium carrier concentration is low at room temperature and thus the on-state resistivity is very high. In order to overcome this problem, solutions based on field effect transistor (FET) are under investigation: Boron δ-doped FET and MOSFET.

3.1. Boron *δ*-doped *FET*

Boron δ-doping consists in a highly doped layer (metallic [B]>5×10^{20} cm^{-3}) between two intrinsic layers, resulting in a conduction combining a high mobility (due to a confinement induced delocalisation of carriers away from the ionized impurities) with a large carrier concentration (due to metallic behaviour). The aim of this work is to investigate the electrical transport properties of the holes confined in the degenerated channel in order to evaluate the potentialities of such structure for high frequency, high power and/or high voltage applications.

The delocalization induced by a quantum confinement of a very thin delta-layer is therefore required, because it allows carriers to be present near the delta-layer due to wave functions extensions. Then a bias on a gate on the surface parallel to the 2D hole gas will allow to modulate the carrier density, and more important, to switch the FET in ‘‘on’’ or ‘‘off’’ state. A diamond field effect transistor based on this delta-doping combines high-speed commutation and low ‘‘on’’ resistance. This structure has been initially proposed for silicon and GaAs devices (for a review, see Ref. [20]), and some experimental realizations have already been reported for diamond [7, 21, 22].

Hall effect and four probes resistivity measurements are the experimental tools generally used to determine the carrier density and mobility in semiconductors. Combined to Secondary Ion Mass Spectrometry, these methods give useful data concerning the activation and ionization of dopants as well as the material quality. In this work, highly doped layers of different thicknesses (from 2 nm to 45 nm of *metallic* thickness) grown on a thick non intentionally doped (*nid*) buffer and covered by another thin *nid* cap layer (from 30 to 65 nm) were investigated by these methods using mesa-etched Hall bars.

From the different samples measurements, two kind of behaviours have been observed: i) a typical metallic conduction with a constant carrier density and a low mobility (μ_h < 10 cm2/V.s) over the whole temperature range, ii) a conduction characterized by a constant mobility and carrier concentration values, which are different in the low temperature range (below T=150 K) and in the high temperature range (above T= 400 K). The sheet carrier density as well as the hole mobility will be discussed in this work and compared to the electrical properties of other wide band gap semiconductor for RF or switch FET application (like AlGaN/GaN HEMT).

3.2. Diamond Metal Oxide Semiconductor capacitance

Achieving an electron inversion layer in a metal oxide semiconductor (MOS) structure is the major obstacle to cross before reaching the fabrication of a MOSFET. For the first time, we reach this result in the case of the diamond. This recent breakthrough suggests the possibility of manufacturing a diamond transistor without being limited by the low ionization rate of the dopants in

the active layer and thus to finally exploit fully the properties of diamond.

In an ideal *p*-type MOS, when a bias voltage is applied to the MOS structure, four regime operations appear. When $V_G<0$, the valence band bends upward and approaches the Fermi level. This band bending causes an accumulation of majority charge carriers at the interface oxide/sc. When $V_G>0$, the valence band moves away from the Fermi level: this is the depletion regime. If the voltage increases further, the curvature increases and the intrinsic Fermi level of the semiconductor just crosses the Fermi level. Conduction at the interface oxide/sc is no longer through the holes but due to electrons that are more numerous: it is the weak inversion regime. The strong inversion is obtained when the gate voltage is enough to get more electrons in the inversion layer than holes in the neutral part of the epilayer (strong inversion regime). All these regimes are well established in Si/SiO_2 MOS capacitance, which is close to the ideal case today (excepted the flat band voltage due to the difference of working function).

For diamond, the different regimes have never been observed due to the poor quality of the interface between the dielectric oxide and the epilayer. The density of states of traps at the interface is too large and when a bias is applied, the traps are charged but no depletion appears. For larger voltage, the breakdown voltage is achieved and no electron inversion can be observed.

In this work, by reducing in an unprecedented way the number of interface states, we succeed to reach the inversion regime in diamond MOS structure. The MOS structure consists of a stack of Al_2O_3/Al gate electrode deposited on a *p*-type epitaxial diamond layer grown on Ib HPHT (100) diamond substrate. An ohmic contact (Ti/Pt/Au annealed at 750 ◦C under vacuum) was also evaporated directly on the epitaxial layer to act as a reference measurement for capacitance measurement. Thanks to the low interface state, the three expected regimes for an ideal MOS structure are observed: i) hole accumulation for $V_G<-4.5V$ ii) depletion (and weak inversion) for $-4.5V<V_G<0.5V$ and iii) inversion (electron) for $V_G >0.5V$. Thanks to this new process (treatment and oxide deposition), we can control the nature of charges at the interface using a gate. This important breakthrough opens the way to the realization of MOS transistor in diamond.

4. SUMMARY

According to the results and analysis presented in this study, it can be concluded that diamond homoepitaxial layers are able to withstand electric fields larger than other wide band gap semiconductors. This property confirms that diamond is the ideal semiconductor for high blocking voltage devices. Schottky diode with blocking voltage up to 10 kV has been reported. The next step will consist to combine such property with a high current density in the forward regime of the diode by using a highly boron doped layer in the stacked structure. Concerning the diamond based field effect transistor, in this work, by reducing in an unprecedented way the number of interface states, we succeed to reach the inversion regime in diamond MOS structure. This funding opens the route to the realization of a diamond MOSFET.

5. REFERENCES

[1] K. Hirama, S. Miyamoto, H. Matsudaira, K. Yamada, H. Kawarada, T. Chikyo, H. Koinuma, K. Hasegawa, H. Umezawa, Appl. Phys. Lett. **88,** 112117 (2006).
[2] K. Hirama, K. Tsuge, S. Sato, T. Tsuno, Y. Jingu, S. Yamauchi, H. Kawarada, Appl. Phys. Express **3**, 044001 (2010).
[3] M. Kasu, H. Sato, and K. Hirama, Appl. Phys. Express **5**, 025701 (2012).
[4] M. Imura, R. Hayakawa, E. Watanabe, M.Y. Liao, Y. Koide, H. Amano, Phys. Status Solidi RRL **5**, 125 (2011).
[5] A. Fiori, J. Pernot, E. Gheeraert and E. Bustarret, Phys. Status Solidi (a) **207,** 2084 (2010).
[6] A. Fiori, G. Chicot, F. Jomard, T. Tran Thi, F. Omnès, E. Gheeraert, E. Bustarret, Diam. Relat. Mater. **24**, 175 (2012).
[7] R.S. Balmer, J.R. Brandon, S.L. Clewes, H.K. Dhillon, J.M. Dodson, I. Friel, P.N. Inglis, T.D. Madgwick, M.L. Markham, T.P. Mollart, N. Perkins, G.A. Scarsbrook, D.J. Twitchen, A.J. Whitehead, J.J. Wilman and S.M. Woollard, J. Phys. Condens. Matter **21,** 364221 (2009).
[8] T. Makino, S. Tanimoto, Y. Hayashi, H. Kato, N. Tokuda, M. Ogura, D. Takeuchi, K. Oyama, H. Ohashi, H. Okushi, and S. Yamasaki, Appl. Phys. Lett. **94**, 262101 (2009).
[9] T. Teraji, S. Koizumi, Y. Koide, and T. Ito, Appl. Surf. Sci. **254**, 6273 (2008).
[10] H. Umezawa, K. Ikeda, N. Tatsumi, K. Ramanujam, and S. Shikata, Diamond Relat. Mater. **18**, 1196 (2009).
[11] P.N. Volpe, J. Pernot, P. Muret and F. Omnès, *Appl. Phys. Lett.* **94**, 092102 (2009).
[12] P.N. Volpe, P. Muret, J. Pernot, F. Omnès, T. Teraji, Y. Koide, F. Jomard, D. Planson, P. Brosselard, N. Dheilly, B. Vergne and S. Scharnholz, *Appl. Phys. Lett.* **97**, 223501 (2010).
[13] P.-N. Volpe, P. Muret, J. Pernot, F. Omnès, T. Teraji, F. Jomard, D. Planson, P. Brosselard, N. Dheilly, B. Vergne, and S. Scharnholtz, Phys. Status Solidi A **207,** 2088 (2010).
[14] G. Chicot, A. Maréchal, P. Muret and J. Pernot, in progress.
[15] M.I. Landstrass, M.A. Plano, M.A. Moreno, S. McWilliams, L.S. Pan, D.R. Kania, and S. Han, Diamond Relat. Mater. **2,** 1033 (1993).
[16] T. Teraji, Y. Garino, Y. Koide, and T. Ito, J. Appl. Phys. **105,** 126109 (2009).
[17] J.E. Butler, M.W. Geis, K.E. Krohn, J. Lawless, Jr., S. Deneault, T.M. Lyszczarz, D. Flechtner, and R. Wright, Semicond. Sci. Technol. **18,** S67 (2003).
[18] P. Muret, J. Pernot, A. Kumar, L. Magaud, C. Mer-Calfati, and P. Bergonzo, Phys. Rev. B **81**, 235205 (2010).
[19] W. Mönch, Europhys. Lett. **27**, 479 (1994).
[20] E. F. Schubert (Ed.), in: Delta-Doping of Semiconductors (Cambridge University Press, Cambridge, 1996).
[21] R.S. Balmer, I. Friel, S.M. Woollard, C.J.H. Wort, G.A. Scarsbrook, S.E. Coe, H. El-Hajj, A. Kaiser, A. Denisenko, E. Kohn, and J. Isberg, Phil. Trans. R. Soc. A **366**, 251 (2008).
[22] H. El-Hajj, A. Denisenko, A. Bergmaier, G. Dollinger, M. Kubovic, and E. Kohn, Diamond Relat. Mater. **17**, 409 (2008).